Research Article

University of Washington
URMSE
Volume 1 (2020)

# Optimization and characterization of printing parameters on a novel continuous carbon fiber composite material for 3D-printing

Sarah Waddell, Esther Law, Amanda Inthavong, Mallory Parker, and Dwayne D. Arola

*Department of Materials Science and Engineering, University of Washington, Seattle, WA 98185, USA*



**Article Info**

Submitted 28 August 2020
DOI: 10.6069/ZDQW-PW89

*Keywords:*
Additive Manufacturing
Carbon Fiber Composites
Thermoplastic

**Abstract**

Additive manufacturing of composites materials is rapidly gaining interest in the aerospace industry due to the technique's flexibility and the high strength to weight ratio of polymer composites. Toray has recently developed a novel continuous carbon fiber (CCF) composite filament with Polyphenylene Sulfide (PPS) resin matrix (CCF/PPS). With a high volume fraction of fibers, 50 $V_f$%, this new filament could introduce significant improvements in mechanical properties upon existing alternatives such as chopped fiber and continuous fiber composites with lower fiber volume fraction. In this investigation, we tested this novel material using fused deposition modeling and quantitatively evaluated the contributions of the printing parameters to the print quality using a Design of Experiments (DOE) approach. The printing parameters included the print height, nozzle temperature, printing speed, and flow rate. We found correlations between the printing parameters to the surface roughness, dimensional accuracy, crystallinity, and microstructure of the printed materials. The resulting printing conditions can be adopted in further scientific investigations as well as serve in the fabrication of high-quality components of this CCF/PPS composite material.

Corresponding author: Esther Law (luoxs98@uw.edu)

## 1. Introduction

Additive manufacturing has become increasingly popular due to its capabilities in customizability, speed, and economic impact. Combining this method with composite materials introduces endless opportunities within the aerospace industry. Today, carbon fiber composites are the preferred material for many aircraft parts because of their high strength, chemical resistance, and lightweight properties [1]. However, traditional carbon fiber composite manufacturing is time-consuming and involves many geometric restrictions to part design. The processing procedure of composite materials often requires a vacuum-bagging method which builds in a layer-by-layer manner using composite prepreg material [2]. The rise of additive manufacturing brings flexibility in design and the possibility of new applications for composites.

Currently, there are some commercially available composite filaments using thermoplastics. Filament made by Markforged is a prime example where composition contains nylon and continuous carbon fiber. This Markforged filament was reported to be 1.4 times stronger and stiffer than Acrylonitrile butadiene styrene (ABS), a common 3D printing plastic [3]. Though this material has improved strength and stiffness, uneven fiber distribution and low volume fraction, around 30 $V_f$ %, have been disadvantageous for aerospace applications. In conventional composite manufacturing methods using vacuum bagging, carbon fiber volume fraction ideally ranges from 30 $V_f$% to 70 $V_f$% [2]. Thus, one way to better the mechanical properties is to increase the volume fraction of carbon fiber. There is also a need for filament with continuous carbon fiber (CCF) to further improve the mechanical properties of 3D printed parts.

A novel composite material for extrusion 3D printing has been developed by Toray Co. that contributes significant advancements to the field of printable aerospace-grade materials. This filament contains continuous carbon fibers

with a volume fraction upwards of 50$V_f$% embedded in a thermoplastic resin.

The purpose of this project is to understand the printing parameter effects on the response and give recommended printing conditions of the Toray CCF filament. However, the quality of printed products is usually influenced by many factors including nozzle temperature, bed temperature, printing speed, Z-height, flow rate or pitch path and so on. With many factors to consider, it becomes difficult to pinpoint which 3D printing parameters produced the optimal part quality. A Plackett Burman design of experiments (DoE) is utilized to study multiple printing parameters and measure multiple print responses while limiting the number of samples used. This method allows a minimal number of tests to be completed while having multiple variables running to determine the impact levels of selected parameters on responses. Employing the Plackett Burman design made studying the significance of each 3D printing factor more efficient for this project.

Previous work in continuous fiber 3D printing done by Matsuzaki et. al provided the basis for the printing process in this project [4], including the printer modification and fiber displacement analysis. In this project, a modified printer design was used to control printing parameters that would otherwise be limited by a standard commercial 3D printer.

## 2. Experimental

### *2.1. Filament and Printer*

This experiment focuses on a novel continuous carbon fiber (CCF) composite filament with Polyphenylene Sulfide (PPS) resin matrix (CCF/PPS) fabricated by Toray with a 50 $V_f$% CCF.

To print this new filament, modifications were made to a commercially available I3 MK3S Prusa 3D printer as shown in **Figure 1**. The altered printer design was based on the continuous filament fiber printer created by the Matsuzaki Group [4]. A specialized printer design was required because Toray did not manufacture this filament to cater to a specific printer. The modifications fell into three general categories: temperature, extrusion, and bed-plate adherence. **Table 1** highlights the attachments added and their purpose on the printer.

### *2.2. Plackett Burman Design of Experiment*

The Plackett Burman design of experiments (DoE) has been commonly used in biotechnology and food industry applications [5]. Two iterations of this design were used in order to evaluate the print parameters and quality.

**Table 1.** Table of the new attachments or replacements for the modified I3 MK3S Prusa Printer.

| Attachment/Part | Reason for Including |
|---|---|
| OMROM Temperature Controller | Allowed for higher nozzle temperatures to be controlled. |
| Extruder | Controls flow rate of the filament via two rollers. |
| PTFE Tubing | Guided the filament to the nozzle during the print. |
| Steel Bed Plate | Allowed for better surface finish and adherence. |

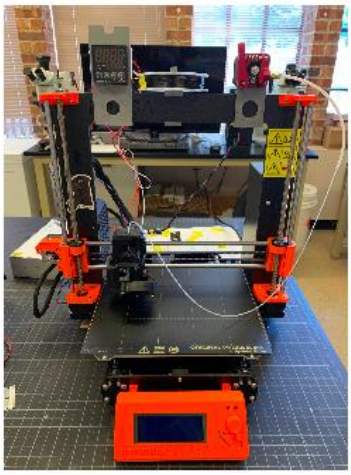

**Figure 1.** Image of modified I3 MK3S Prusa printer.

#### *2.2.1. Primary Plackett Burman Design of Experiment*

The first objective was to rank the independent print parameters to gain a qualitative understanding of the factor influence. Out of the possible parameters, six were selected for the primitive Plackett Burman Design, including nozzle temperature, bed temperature, Z-height, print speed, flow rate, and path pitch. In order to set up a full Plackett Burman design, an 8-by-2 matrix with high and low levels with various combinations of each parameter was created. The measured variables of print quality were rated qualitatively by best human judgment for surface roughness and side-by-side filament adhesion. The first primitive result showed that four factors: nozzle temperature, Z-height, print speed, and flow rate had a higher influence on the printed sample quality. A secondary Plackett Burman design of the experiment was then used to study these four parameters in more depth.

#### *2.2.2. Secondary Plackett Burman Design of Experiment*

The second iteration of the Plackett Burman design investigated the level of dependency of printing parameters on the responses. The four printing factors which were selected from the first round DoE can be observed in **Table 2**. A 3D printed sample is considered the 'best print' if it has minimal surface roughness, accurate dimension thickness, maximum crystallinity, and even fiber distribution (**Table 3**). By quantifying these responses, we were able to calculate the estimated effect of each factor visualized through scree plots. Nine printed samples were used at three different levels of varied factors in order to satisfy a 3-by-9 matrix, leading to a total of 27 samples. The three levels of variation used for each factor can be seen in **Table 2**.

### *2.3. Physical Characterization*

The four parameters of interest were tested for all 27 samples. These samples were printed with Toray's filament as a single layer consisting of 5 rows of filament with set dimensions of 50 mm by 14.5 mm. The bed temperature was maintained at 90°C throughout the experiment.

**Table 2**. Print factors and variation range used in DoE.

| | Factors | Low (-) | Mid (0) | High (+) |
|---|---|---|---|---|
| A | Nozzle Temp. (℃) | 310 | 330 | 345 |
| B | Z-Height (mm) | 0.20 | 0.35 | 0.50 |
| C | Print Speed (mm/min) | 150 | 250 | 350 |
| D | Flow Rate (%) | 50 | 55 | 60 |

**Table 3**. Goals for each optimal response.

| Response | Goal |
|---|---|
| Surface Roughness | Minimize |
| Dimension Accuracy | Target |
| Crystallinity | Maximize |
| Fiber Placement | Target |

Surface roughness is essential to evaluate manufacturing and product finish. Surface roughness is defined in this work as the absolute value of the extension of arithmetical mean height to the reference surface [6]. A print with minimal surface roughness is preferable for a good surface finish since less surface defects are present. A Keyence optical profilometer was used to determine the surface roughness.

Dimensional accuracy was an important response to consider in validating the quality of a print. Length, width and thickness of the prints were measured using an electronic caliper and compared to target dimensions. From the measurements collected, the percent error was calculated relative to the ideal dimensions.

Thermal analysis was done using differential scanning calorimetry (DSC) with TA Instruments DSC Q20. In order to determine the degradation temperature, the samples were tested using thermogravimetric analysis (TGA) before running DSC. Unprinted CCF filament samples analyzed in TGA exhibited a ramp rate of 20°C/min until 860°C, revealing a degradation temperature of around 500°C. When preparing sections for DSC trials, small sections of 5mg ±0.2mg were cut out from each sample and placed in designated aluminum Tzero pans.

To measure the level of fiber dispersion, MatLab was used to identify the location of each fiber. Cross-sectional images of printed samples were taken perpendicular to the CF direction using visible light microscopy. From the resulting images, the filament was isolated within a mask and put on a grayscale to accentuate the CF fibers from the surrounding matrix. Each small, circular region was identified as a fiber. The pixels within each fiber region were counted by the program and taken as a ratio from the total pixels within the isolated mask, or fiber boundary. A location is also assigned to the center of each fiber, allowing the program to track them individually.

## 3. Results and discussion

### *3.1 Filament Morphology*

**Figure 2** shows the cross-section images of as-is or unprinted filaments of Markforged Nylon-CCF and Toray. As compared between the microscopic images, the volume fraction of the novel Toray filament is significantly higher than the commercial Markforged filament. Furthermore, the fiber volume fraction was calculated using the Matlab code that counts individual fibers on the cross-section. Based on the calculations, the average fiber volume fraction for Toray and Markforged Nylon-CCF filaments were 41.25±2.22 $V_f$% and 27.5±6.30 $V_f$% respectively.

### *3.2 Surface roughness*

Keyence profilometer measurements were taken from three distinct areas on each sample with the average representing the surface roughness. As seen in **Figure 3**, the red area indicates the maximum height and the blue area represents the minimum height. The surface roughness of 27 printed samples had values ranging from 10-180 μm. The worst quality print (**Figure 3a**) was quantified with 3D surface roughness around 180 μm, while the best quality (**Figure 3b**) was closer to 10 μm. The surface roughness data were collected and analyzed for scree plots.

### *3.3 Dimensional Accuracy*

While the width and length measurements were generally consistent, the error between printed and target dimension was primarily due to thickness. This is best highlighted in **Figure 4**, showing the percent error contributed by thickness, length, and width compared to the overall total error. The total error is the summation of the percent errors from all three dimensions. Thickness clearly presents itself as a major influence in percent error as it is similar in values for the total error. The values for length and width remained close to zero, showing a lack of contribution to the total percent error.

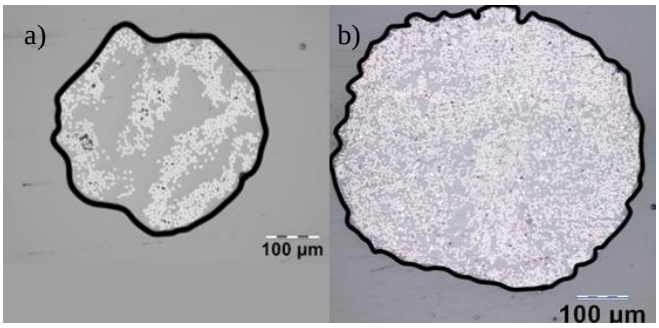


**Figure 2.** Images from cross-sectional areas for As-Is unprinted filament for a) Markforged Nylon-CCF and b) Toray filament.

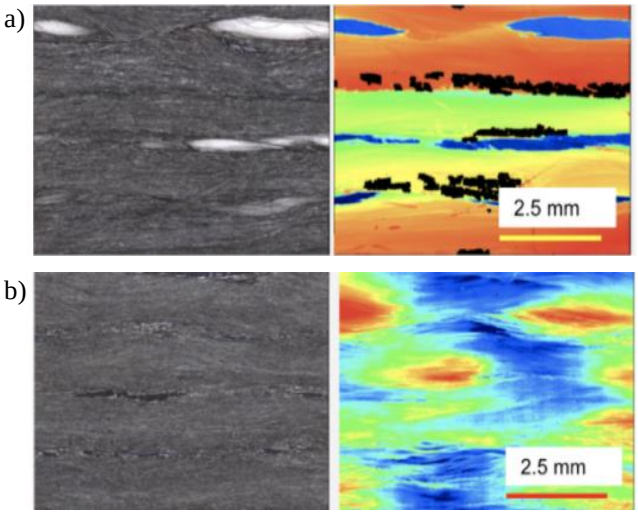


**Figure 3.** Microscopic images and heat graphs of samples printed with b) high nozzle temperature and Z-height, middle print speed, low flow rate.

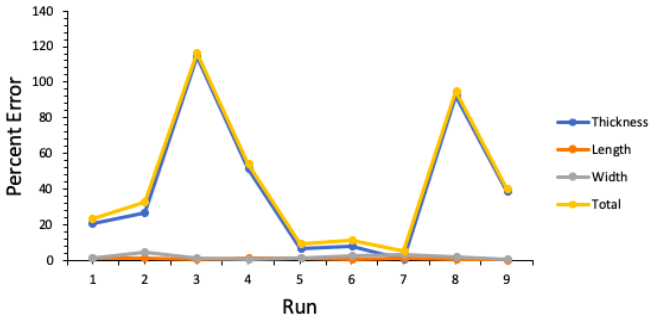


**Figure 4.** Total Percent Error-values corresponding with the Plackett Burman runs.

### *3.4 Crystallinity*

Running a thermal cycle (**Figure 5)** revealed the melting temperature and crystallization temperature of PPS. The percent crystallinity was then calculated using **equation 1**. Here, $\Delta H_m$and $\Delta H_c$ are the enthalpies in J/g at the melting point and cold crystallization point respectively. These values were calculated as the area under the curve from the DSC data. As indicated in **equation 2**, the $W_f$ is the mass fraction of CF to the entire filament. In order to find the CF mass, the CF volume fraction ($V_f$) was calculated from the CF fiber count and radius. The CF density, $\rho_{CF}$ , was provided by Toray and the value for $\Delta H_m^o$ was used from Maemura et. al [7].

$$X_m = \frac{\Delta H_m - \Delta H_c}{(1 - W_f) * \Delta H_m^o} \quad (1)$$

$$W_f = \frac{\rho_{CF} * V_f}{Filament\ Section\ Mass} \quad (2)$$

As seen from the DSC curves (**Figure 5**), the sample printed at the highest nozzle temperature of 345°C showed the largest curve at the cold crystallization temperature. This heightened peak results in a decreased percent crystallinity. Virgin PPS, on the other hand showed a much higher curve at the melting point, increasing the value and corresponding higher percent crystallinity. These results show a possible correlation between higher nozzle temperature and lower crystallinity.

### *3.5 Fiber Distribution*

Fiber distribution was analyzed from the cross-sectional images of the printed filament as seen in **Figure 6a**. These were then analyzed using the MatLab code as mentioned in *Section 2.3 Physical Characterization*. In order to quantify the fiber distribution for each sample, graphs were generated displaying the distance of each fiber to the bottom of the entire filament in a histogram. This can be seen in **Figure 6b**, where the frequency of fibers is shown for each increment of distance. An even distribution of fibers is indicated by a slope of zero where the line appears horizontal. Hence, a flatter or smaller slope value can predict a more even fiber distribution within a sample.

### *3.6 Plackett Burman Discussion: Scree Plots*

The Plackett Burman DoE allows conclusions to be drawn from plotting the estimated effect of each print parameter. From the previous set of experiments, data was collected for the response of each sample in the form of surface roughness value, dimensional percent error, percent crystallinity, and fiber distribution slope. Each of these responses were multiplied by the designated contrast values (ranging from -1 to 1) which were pre-determined from using the 3-by-9 matrix [5]. Adding up their products results in a contrast value for each of the four print parameters, which were used to calculate the sum of squares. After normalization, the estimated effect was determined which represents the parameters' overall impact on samples within one of the levels: low, middle or high. The estimated effects for each level are plotted in **Figure 7**, representing the DoE results in four graphs or scree plots.

The parameters with high estimated effects indicate a larger influence on the response or quality. Consistency between low, middle, and high levels for one factor is ideal for the scree plots because this signifies that a factor is the

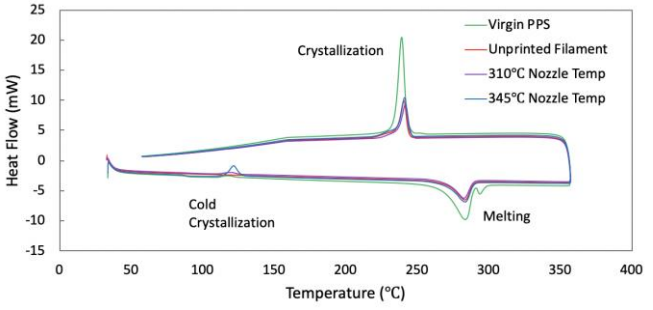


**Figure 5.** DSC curves comparing pure PPS, unprinted filament, and printed filament at different temperatures.

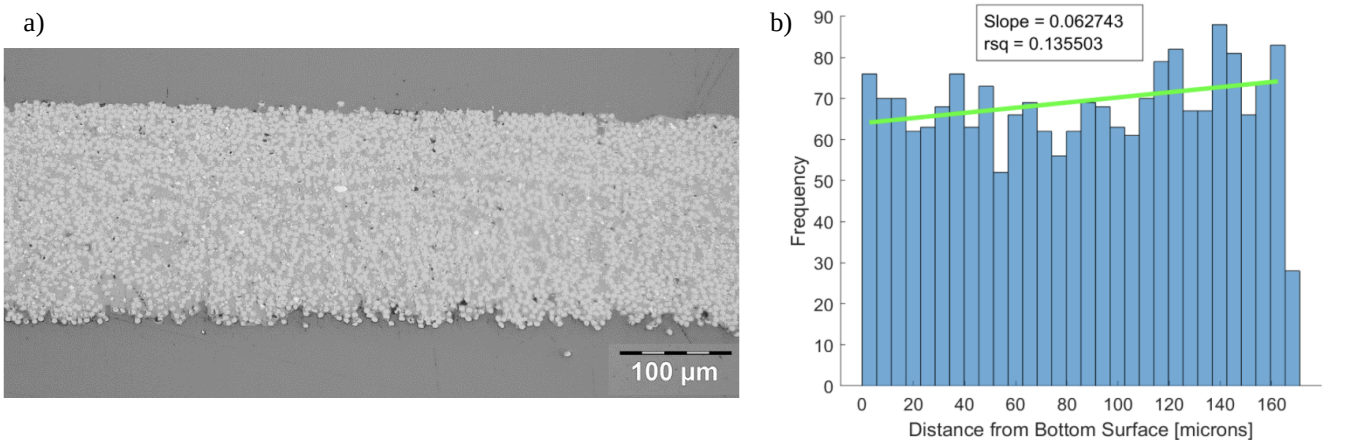


**Figure 6.** a) Cross-section of the sample taken by light microscope showing fiber distribution. b) Histogram depicting the changing frequency in carbon fiber distribution.

primary influence on a response. The scree plots of surface roughness and crystallinity both exhibit identical trends of significance among levels. As seen in the surface roughness scree plot, Z-height greatly impacted surface roughness in all three levels. The other three factors showed minimal effects on surface roughness. This indicates that minimal surface roughness can be found in conditions with controlled Z-height. For thickness dimensional accuracy, it was shown that low nozzle temperature and high flow rate resulted in accurate thickness. In addition, the highest crystallinity was found in medium-low print speed and low nozzle temperature. For fiber displacement response, the result showed that medium-low Z height and high flow rate contributed most for even carbon fiber distribution. These scree plots could be used to visualize the printing factor effects on the resulting responses.

In some cases, results are not consistent among the three levels (e.g. the thickness dimensional accuracy plot), indicating that more than one parameter may be affecting this response. This can be understood as secondary affecting parameters, which would require further analysis and experimentation to identify.

## 4. Conclusions

A printable composite material was recently developed by Toray with a high volume fraction of continuous carbon fiber in a PPS resin matrix. The purpose of this paper was to evaluate the printability of this novel material and eventually help suppliers improve manufacturing methods to further develop this material. As specified, a preliminary Plackett Burman Design of Experiments was conducted to evaluate

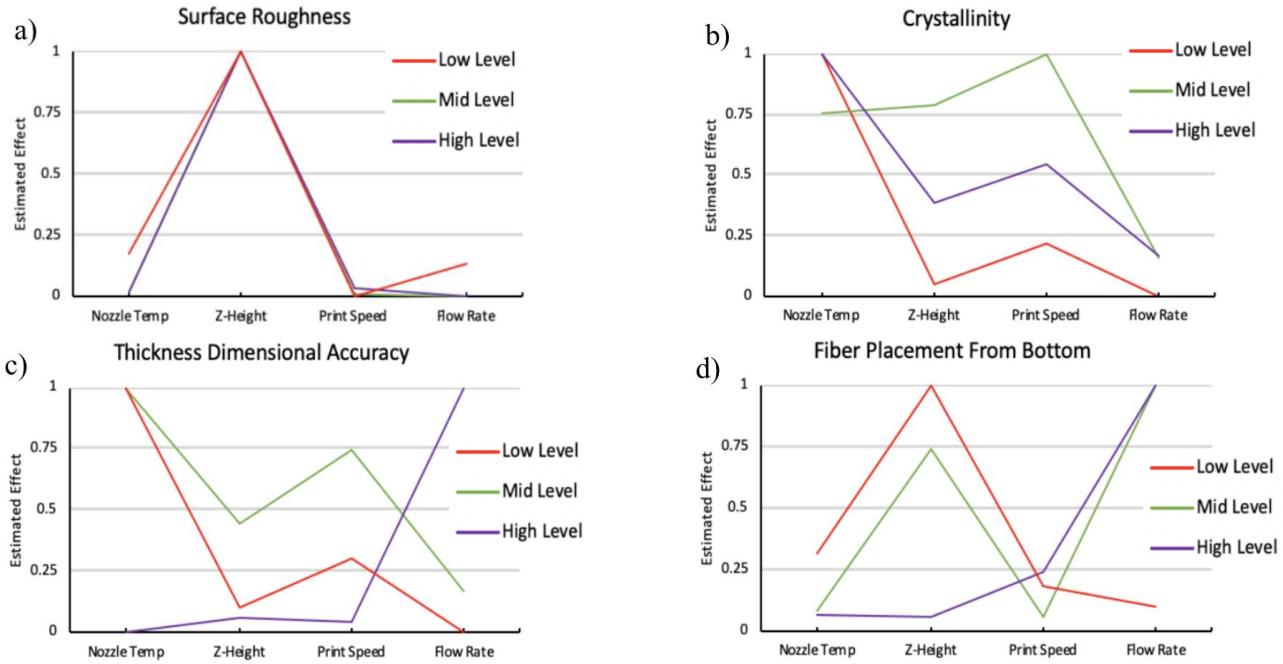


**Figure 7** Estimated effect of nozzle temperature, z-height, print speed, and flow rate on responses in three levels of surface roughness (a), crystallinity (b), dimensional accuracy (c), and fiber placement (d).

common printing factors including nozzle temperature, Z-height, bed temperature, path pitch, print speed and flow rate on the quality of the prints. The preliminary Plackett Burman design of experiment successfully narrowed down to four impacting printing parameters, which are nozzle temperature, Z-height, print speed, and flow rate. Using this information, the second iteration of DoE testing was conducted to understand the significance of printing parameters on four specific sample responses, which included surface roughness, accuracy of thickness dimension, crystallinity, and carbon fiber distribution within the filament.

To summarize and draw primitive conclusions from the scree plots from Plackett Burman Design, a list of optimal printing parameters can be found in **Figure 8**. This novel continuous carbon fiber composite with high volume fraction carbon fiber can be printed with the recommended settings combinations below to achieve high printing quality.

## Acknowledgements

This work was conducted within the D. Arola Group at the University of Washington, Seattle, in collaboration with the R. Matsuzaki Group from the Tokyo Institute of Technology, Japan. Sponsorship was provided by JCATI and Toray Co.

## Conflict of Interest

No conflict of interest.

## References

[1] K. Chawla, *Carbon Fiber/Carbon Matrix Composites. In Composite Materials: Science and Engineering*, 3rd ed. New York, NY: Springer New York, 2012.

[2] D.M. Rachal, J.R. Krove, "Vacuum bagging process for fiber reinforced thermoplastics", United States Patent 4915896, Apr. 10, 1990.

[3] The Markforged Corporation, "*Composites Material Datasheet*," Watertown MA, USA, 2019. Accessed on: June 8, 2020. Available: http://static.markforged.com/downloads/composites-data-sheet.pdf

[4] R. Matsuzaki, T. Nakamura, K. Sugiyama, M. Ueda, A. Todoroki, Y. Hirano, and Y. Yamagata, *"Effects of Set Curvature and Fiber Bundle Size on the Printed Radius of Curvature by a Continuous Carbon Fiber Composite 3D Printer,"* Additive Manufacturing, vol. 24, pp. 93-102, 2018.

[5] R.L. Plackett and J.P. Burman, "*The Design of Optimum Multifactorial Experiments*", Biometrika. vol. 33, no. 4, pp. 305–325, June 1946. doi:10.1093/biomet/33.4.305

[6] "Area Roughness Parameter: surface texture parameter in ISO 25178" Keyence. [Online] Accessed on: June 8, 2020, Available: https://www.keyence.com/ss/products/microscope/roughness/surface/parameters.jsp?fbclid=IwAR3eyy5dX-6pHuprq5DyNeU4Um-fww2LbH8fAuQ78AxX_EOPwSLfvsPoMYo

[7] E. Maemura, M. Cakmak, and J. White, "*Characterization of crystallinity, orientation, and mechanical properties in biaxially stretched poly(p-phenylene sulfide) films*." Polymer Engineering And Science, vol. 29, no. 2, pp. 140-150. 1989.